Video Article

Rapid, Scalable Assembly and Loading of Bioactive Proteins and Immunostimulants into Diverse Synthetic Nanocarriers Via Flash Nanoprecipitation

Sean Allen[1], Michael Vincent[1], Evan Scott[1,2]

[1]Interdisciplinary Biological Sciences, Northwestern University

[2]Department of Biomedical Engineering, Northwestern University

Correspondence to: Evan Scott at evan.scott@northwestern.edu

URL: https://www.jove.com/video/57793
DOI: doi:10.3791/57793

Keywords: Bioengineering, Issue 138, nanomaterial, nanocarrier, biomaterial, controlled delivery, self-assembly, flash nanoprecipitation, fabrication, polymer, block copolymer

Date Published: 8/11/2018

Citation: Allen, S., Vincent, M., Scott, E. Rapid, Scalable Assembly and Loading of Bioactive Proteins and Immunostimulants into Diverse Synthetic Nanocarriers Via Flash Nanoprecipitation. *J. Vis. Exp.* (138), e57793, doi:10.3791/57793 (2018).

Abstract

Nanomaterials present a wide range of options to customize the controlled delivery of single and combined molecular payloads for therapeutic and imaging applications. This increased specificity can have significant clinical implications, including decreased side effects and lower dosages with higher potency. Furthermore, the *in situ* targeting and controlled modulation of specific cell subsets can enhance *in vitro* and *in vivo* investigations of basic biological phenomena and probe cell function. Unfortunately, the required expertise in nanoscale science, chemistry and engineering often prohibit laboratories without experience in these fields from fabricating and customizing nanomaterials as tools for their investigations or vehicles for their therapeutic strategies. Here, we provide protocols for the synthesis and scalable assembly of a versatile non-toxic block copolymer system amenable to the facile formation and loading of nanoscale vehicles for biomedical applications. Flash nanoprecipitation is presented as a methodology for rapid fabrication of diverse nanocarriers from poly(ethylene glycol)-*bl*-poly(propylene sulfide) copolymers. These protocols will allow laboratories with a wide range of expertise and resources to easily and reproducibly fabricate advanced nanocarrier delivery systems for their applications. The design and construction of an automated instrument that employs a high-speed syringe pump to facilitate the flash nanoprecipitation process and to allow enhanced control over the homogeneity, size, morphology and loading of polymersome nanocarriers is described.

Video Link

The video component of this article can be found at https://www.jove.com/video/57793/

Introduction

Nanocarriers allow for the controlled delivery of small and macromolecular cargo, including active entities that, if not encapsulated, would be either highly degradable and/or too hydrophobic for administration *in vivo*. Of the nanocarrier morphologies regularly fabricated, polymeric vesicles analogous to liposomes (also called polymersomes) offer the ability to simultaneously load hydrophilic and hydrophobic cargo[1,2]. Despite their promising advantages, polymersomes are still rare in clinical applications due, in part, to several key challenges in their manufacturing. For clinical use, polymersome formulations need to be made in large-scale, sterile, and consistent batches.

A number of techniques can be used to form polymersomes from a diblock copolymer, such as poly(ethylene glycol)-*block*-poly(propylene sulfide) (PEG-*bl*-PPS), that include solvent dispersion[3], thin film rehydration[1,4], microfluidics [5,6], and direct hydration[7]. Solvent dispersion involves long incubation times in the presence of organic solvents, which may denature some bioactive payloads, like proteins. Thin film rehydration does not offer control over the polydispersity of the formed polymersomes, often requiring expensive and time-consuming extrusion techniques to achieve acceptable monodispersity. Furthermore, both microfluids and direct hydration are difficult to scale up for larger production volumes. Of the different nanocarrier fabrication methods, flash nanoprecipitation (FNP) offers the ability to make large-scale and reproducible formulations[8,9,10]. While FNP was previously reserved for the formulation of solid-core nanoparticles, our lab has recently expanded the use of FNP to include the consistent formation of diverse PEG-*bl*-PPS nanostructure morphologies[11,12], including polymersomes[11] and bicontinuous nanospheres[12]. We found that FNP was capable of forming monodisperse formulations of polymersomes without the need for extrusion, resulting in superior polydispersity index values compared to non-extruded polymersomes formed by thin film rehydration and solvent dispersion[11]. Bicontinuous nanospheres, with their large hydrophobic domains, were not able to be formed by thin film rehydration, despite forming under a number of solvent conditions with FNP[12].

Here, we provide a detailed description for the synthesis of the PEG-*bl*-PPS diblock copolymer used in polymersome formation, the confined impingement jets (CIJ) mixer used for FNP, the FNP protocol itself, and the implementation of an automated system to reduce user variability. Included is information on how to sterilize the system sufficiently to produce endotoxin-free formulations for use *in vivo*, and representative data concerning the characterization of polymersomes formed by FNP. With this information, readers with interest in utilizing polymersomes for *in*

Copyright © 2018 Journal of Visualized Experiments

vitro and *in vivo* work will be able to fabricate their own sterile, monodisperse formulations. Readers with experience in nanocarrier formulations and with polymer synthesis expertise will be able to rapidly test their own polymer systems using FNP as a potential alternative to their current formulation techniques. Additionally, the protocols described herein may be used as educational tools for the formulation of nanocarriers in nanotechnology laboratory courses.

Protocol

1. Synthesis of Poly(ethylene glycol)-*block*-poly(propylene sulfide)-Thiol

1. Synthesize methoxy-poly(ethylene glycol) mesylate (Mn: 750) (MeO-PEG_{17}-Ms, **I**).
    1. Dissolve 10 g of MeO-PEG_{17}-OH in 200 mL of 100% toluene within a 3-neck round bottom flask (RBF) under magnetic stirring at 600 rpm.
    2. Connect the 3-neck RBF to a Dean-Stark apparatus, itself attached to a condenser, keep the entire system under inert gas, either nitrogen or argon.
    3. Place the 3-neck RBF in an oil bath, heat to 165 °C while stirring at 600 rpm.
    4. Remove trace water and 100 mL of toluene using azeotropic distillation.
    5. Remove the 3-neck RBF from oil, detach the Dean-Stark apparatus while maintaining inert gas conditions, and allow to cool to room temperature.
    6. Add 5.6 mL of 100% triethylamine (3 molar eq.) and 300 mL of anhydrous 100% toluene to MeO-PEG_{17}-OH solution while stirring at 600 rpm.
    7. Move the 3-neck RBF to an ice bath, maintain stirring at 600 rpm and inert gas conditions.
    8. Dilute 3.1 mL of 100% methanesulfonyl chloride (3 molar eq.) in 30 mL of 100% toluene, slowly add to the 3-neck RBF via an addition funnel while stirring at 600 rpm.
    9. Stir overnight at 600 rpm at room temperature under inert conditions.
    10. Filter solution through a Buchner funnel packed with diatomaceous earth (see **Table of Materials**) to remove salts.
    11. Remove toluene via a rotary evaporator with the water bath set to 40 °C, rotation at 120 rpm, and pressure set to between 50-100 millibar.
    12. Re-dissolve product in 200 mL of 100% dichloromethane (DCM), and filter through a Buchner funnel packed with diatomaceous earth (see **Table of Materials**).
    13. Remove DCM via a rotary evaporator with the water bath set to 40 °C, rotation at 120 rpm, and pressure set to between 450-600 millibar.
    14. Sparingly re-dissolve product in 100% DCM and slowly precipitate product by adding it dropwise (via Pasteur pipette) to 500 mL of ice-cold 100% diethyl ether. Maintain stirring at 300 rpm.
    15. Decant or aspirate to remove diethyl ether from precipitated product, MeO-PEG_{17}-Mesylate, and store overnight in vacuum desiccator to dry completely.
    16. Use product immediately, or store under inert gas at -20 °C for several months.

2. Synthesize methoxy-poly(ethylene glycol) thioacetate (MeO-PEG_{17}-TA, **II**).
    1. Dissolve 5 g of MeO-PEG_{17}-Ms **(I)** in 200 mL of 100% anhydrous dimethylformamide (DMF) in a 3-neck RBF, stir at 600 rpm at room temperature under inert gas.
    2. Add 2.5 g of 100% potassium carbonate (3 molar eq.) to stirring solution.
    Note: Potassium carbonate will not completely dissolve in solution.
    3. Dilute 1.3 mL of 100% thioacetic acid (3 molar eq.) in 100 mL of 100% anhydrous DMF, and add dropwise to solution via an addition funnel.
    Note: Thioacetic acid has a strong, displeasing odor. Care must be taken to keep all soiled objects within the chemical fume hood overnight prior to disposal or cleaning.
    4. Stir vigorously (rpm 600 or greater) overnight at room temperature.
    Note: Salt formation can easily disrupt the stirring of this solution. Care must be taken to maintain stirring overnight.
    5. Filter solution through a Buchner funnel packed with diatomaceous earth (see **Table of Materials**).
    6. Remove DMF via a rotary evaporator with the water bath set to 60 °C, rotation at 120 rpm, and pressure set to between 5-15 millibar.
    7. Dissolve product in 100 mL of 100% tetrahydrofuran (THF) and add to a column packed with neutral alumina to remove red/orange colored impurities.
    8. Remove THF via a rotary evaporator with the water bath set to 40 °C, rotation at 120 rpm, and pressure set to between 200-300 millibar.
    9. Sparingly re-dissolve product in 100% DCM. If a salt precipitate forms, filter solution through 6 µm pore size filter paper using a Buchner funnel.
    10. Slowly precipitate product by adding dropwise via Pasteur pipette to 500 mL of ice-cold 100% diethyl ether, stirring at 300 rpm. Diethyl ether may need to be further chilled to -20 °C in an explosion-proof freezer for several hours if precipitate does not crash out of solution at 4 °C.
    11. Decant or aspirate to remove diethyl ether from precipitated product, MeO-PEG17-Thioacetate. Store product overnight in a vacuum desiccator, and subsequently under inert gas at -20 °C.

3. Synthesize diblock copolymer poly(ethylene glycol)-*block*--poly(propylene sulfide)-thiol (PEG_{17}-*bl*-PPS_{35}-SH, **III**).
    1. Dissolve MeO-PEG_{17}-TA **(II)** in 10 mL of 100% anhydrous DMF within a Schlenk flask under argon, while stirring at 400 rpm in a room temperature water bath.
    2. Add 1.1 molar eq of sodium methoxide (0.5 M solution in methanol), allow to stir at 400 rpm for 5 minutes.
    3. Add 35 molar eq of 100% propylene sulfide, rapidly, to solution. Allow to stir at 400 rpm for 10 minutes.
    4. Add 10 molar eq of 100% glacial acetic acid, allow to stir at 400 rpm for 5 minutes.

Copyright © 2018 Journal of Visualized Experiments

5. Remove DMF via a rotary evaporator with the water bath set to 60 °C, rotation at 120 rpm, and pressure set to between 5-15 millibar.
6. Re-dissolve product sparingly in 100% DCM, precipitate in 80 mL of 100% methanol, split between two 50 mL conical centrifuge tubes.
7. Centrifuge conical tubes at 7500 x g for 5 minutes at 4 °C. Aspirate away supernatant.
8. Store product, PEG_{17}-*bl*-PPS_{35}-SH, overnight in a vacuum desiccator, and subsequently under inert gas at -20 °C.

2. Assemble PEG-*bl*--PPS Nanocarriers via Hand-Powered Flash Nanoprecipitation

1. (Optional) Sterilize the confined impingement jets (CIJ) mixer.
    1. Within a biological safety cabinet (BSC), submerge mixer with all parts disassembled within 0.1 M NaOH overnight.
    2. Reassemble CIJ mixer, and flow through endotoxin-free water using luer-lock syringes.
    3. Test the pH of the water, and continue to flow water through until pH registers as neutral.

2. Dissolve PEG_{17}-*bl*-PPS_{35}-SH polymer and hydrophobic cargo in THF (impingement solution 1).
    1. Weigh 20 mg of PEG_{17}-*bl*-PPS_{35}-SH into a 1.5 mL tube.
    2. Add hydrophobic dyes (*e.g.,*DiI, ICG), drugs (*e.g.,*rapamycin), or other cargo.
    Note: Cargo may be dry, or dissolved in a water-miscible solvent, preferably THF. If cargo is insoluble in THF or DMF, another water-miscible solvent may be used, but sparingly, as the polymer is unlikely to be soluble. The amount of cargo that can be loaded is dependent on the cargo properties itself (*e.g.,* the molecular weight, the hydrophobicity, steric considerations), and should be explored on a case-by-case basis[11,12].
    3. Add 500 µL of 100% THF to the polymer and cargo, vortex vigorously to dissolve.

3. Dissolve hydrophilic cargo in aqueous buffer (impingement solution 2). For this, dissolve hydrophilic cargo to be loaded within polymer vesicles in 500 µL of an aqueous buffer (*e.g.,* phosphate-buffered saline, pure water, *etc.*) as needed.
4. Add buffer to reservoir.
    1. Add 2.5 mL of an aqueous buffer of choice (*e.g.,* 1x phosphate buffered saline) to a suitably sized reservoir (*e.g.,* a 20 mL glass scintillation vial). Place reservoir under CIJ mixer such that the outflow from the mixer directly enters the reservoir.

5. Load impingement solutions into separate 1 mL plastic disposable syringes.
6. Impinge solutions against each other to simultaneously form nanostructures and load them with the payload.
    1. Insert syringes into Luer-lock adapters at the top of the CIJ mixer.
    2. In a single, smooth, and rapid motion, depress both syringes simultaneously and with equal force.
    Note: If performing multiple sequential impingements, first collect outflow in an empty reservoir.
    3. (Optional) Perform multiple impingements. Split nascent nanostructure solution between two syringes, and repeat steps 2.6.1-2.6.2 up to 4 more times.
    4. Collect outflow in the aqueous buffer-filled reservoir prepared in 2.4.1 and gently stir to ensure mixing.

7. Remove unloaded cargo and organic solvent.
    1. (Option 1) Dialyze nanocarrier formulation in the same aqueous buffer used for impingement and in the reservoir, using tubing of an appropriate MW cutoff for at least 24 hours with at least 2 buffer changes. This can be performed at room temperature.
    Note: Nanocarriers will be retained by tubing with a MW cutoff <100,000 kDa and may potentially be retained by higher cutoffs as well. This option maintains sterility when performed in a BSC using sterile buffer.
    2. (Option 2) Filter formulation through a size exclusion or desalting/buffer exchange column (*e.g.,* Sepharose 6B column) using 1x PBS as the aqueous buffer.
    Note: This option maintains sterility when performed in a BSC with a column that has been thoroughly sterilized.
    3. (Option 3) Remove volatile organic solvent using vacuum desiccation overnight.
    4. (Option 4) Filter formulation using a tangential flow filtration system using a 50-100 kDa filter at a 20-60 mL/min flow rate for 15 minutes to 1 hour, depending on the molecular weight of the unencapsulated cargo being purified away (larger cargo will take longer).

8. (Optional) Concentrate the nanocarrier formulation.
    1. (Option 1) Concentrate using a spin concentrator system (*e.g.,* spin column with MW cutoff > 100,000), used as described by manufacturer.
    Note: Nanocarriers may need to be resuspended between spins and may require a number of spins to concentrate down to desired volume. Spin concentration may reduce sterility of nanocarrier formulations.
    2. (Option 2) Reduce volume using vacuum desiccation.
    Note: Volume change is difficult to control under these conditions, and care must be taken to maintain osmolarity before and after concentration.

9. Store nanocarriers at 4 °C for weeks to months. Prior to use after storage, briefly vortex nanocarrier formulations.

3. Characterize Nanocarrier Formulations

1. **Measure loading efficiency**
    1. If cargo is fluorescent or absorbs strongly at a given wavelength outside of 260-450 nm, measure fluorescence/absorbance using a fluorimeter/spectrophotometer.
    Note: PEG-*bl*-PPS absorbs strongly from 260-310 nm and polymersome formulations absorb from 310-450 nm, which may complicate quantification of cargo that absorbs at a similar wavelength.
    2. If cargo absorbs within the 260-450 nm range and is hydrophilic, disrupt PEG-*bl*-PPS nanostructures by adding 25 µL of the formulation to an equal volume of either 1% H_2O_2 or 1% Triton X-100 and subsequently separate and distinguish cargo from polymer absorbance

via high-performance liquid chromatography (HPLC) using a size exclusion column compatible with aqueous buffers (*e.g.,* a Sepharose 6B column) [11].

3. If cargo absorbs within the 260-450 nm range and is soluble in THF or DMF, lyophilize the formulation by freezing 100 µL in a 1.5 mL plastic tube at -80 °C overnight. Then place the tube into a glass vacuum container and place onto a lyophilizer. Allow 24 hours for lyophilization to occur and subsequently re-dissolve in 50 µL of DMF or THF prior to separation and detection via HPLC.

2. **Measure nanocarrier size and morphology**
   1. Use dynamic light scattering (DLS)[11] or nanoparticle tracking analysis[13] to measure nanocarrier size.
      Note: Nanocarriers formed from PEG_{17}-*bl*-PPS_{35}-SH are expected to have an average diameter between 100-200 nm, with a polydispersity index < 0.3.
   2. Determine nanocarrier morphology using cryogenic transmission electron microscopy (cryoTEM)[14].
      Note: Nanocarriers formed from PEG_{17}-*bl*-PPS_{35}-SH are expected to be polymer vesicles (polymersomes) with a clearly discernable polymeric membrane and largely spherical shape.

3. **(Optional) Test formulations for endotoxin**
   1. (Option 1) Use a cell-based assay for the presence of endotoxin, *e.g.,* RAW Blue cells or HEK Blue TLR4 cells (see **Table of Materials**), as described by manufacturer, in either a quantitative or qualitative assay for lipopolysaccharides (LPS)[13].
   2. (Option 2) Use a Limulus Amebocyte Lysate (LAL)[15] assay kit, as described by the manufacturer.

4. Fabrication of a high-speed syringe pump for FNP

1. Fabricate custom instrument components.
   Note: 3D models for machining all custom parts are provided in supplementary materials.
   1. Machine multi-layered instrument chassis from ¾" acrylic sheets and assemble (see **Supplementary Files 1-5**).
      Note: Acrylic has poor chemical resistance. If the instrument is to be used with harsh solvents, machine the base from a metal deemed suitable for the application.
   2. 3D print parts with printed with polylactide (PLA) plastic.
      1. Print the syringe expulsion (SE) 2-part apparatus: SE part 1 - Rear FNP block holding carriage (**Figure 5F**, gray part; **Supplementary File 6**) and SE part 2 - Front Expulsion guide (**Figure 5F**, black part; **Supplementary File 7**). See **Supplementary File 2** for schematics.
      2. Print the infrared sensor braces (**Figure 5I**, black boxes; **Supplementary Files 8 and 9**).
      3. (Optional) Print the dual syringe plunger brace.

2. Fasten instrument chassis layers together with M5 hex bolts and add rubber feet to the base.
3. Configure a single-board computer with the Raspbian GNU/Linux 8.0 (Jessie) operating system (based on Linux Debian).
   Note: Software for operating the Instrument is available upon request. Instrument software source code available upon request. Upon receiving zipped file, download all dependencies specified in the README file. This software includes a simple graphic user interface that enables control over instrument operation, including basic run parameters (motor speed, direction, *etc.*). Users are encouraged to expand on the existing source code and program custom modules tailored for use in their own experiments. All software was written using Python 2.7.12 and is not currently compatible with Python 3. RPi, PicoBorgRev, kivy, and multiprocessing modules are utilized. The README file contains detailed information regarding the software distribution license.
4. Install a 24 V brushed DC motor (**Figure 5A**) and precision slide (4.5" (114.3 mm) stroke; 1.27 mm screw lead) (**Figure 5C**).
   Note: The 24 V DC motor used here has a RPM_{max}, I_{max}, and full-load torque of 4,252 RPM, 4.83 A, and ~0.2 N*m, respectively.
   1. (Optional) Place padding underneath the motor to dampen vibration during operation.
      Note: It is recommended that a 2-3 mm thick rubber pad is cut to fit the motor carriage dimensions of the instrument base.
   2. Mount the precision slide to the instrument base.
      1. Remove the threaded rod temporarily.
      2. Mount slide using two #8-32 flat machine screws.
   3. Mount DC motor to precision slide using screw beam coupling (1-1/4" length) containing 6/16" and 1/4" diameter bores.
      Note: Depending on the thickness of acrylic used to machine the instrument base layers, shims may be needed to level the motor and precision slide shafts.

5. Assemble expulsion platform from metal plates and L-shaped corner braces (**Figure 5D**). Mount base metal platform to sliding platform (attached to threaded rod) using #6-32 screws. See precision slide schematic provided by manufacturer for details regarding the mounting constraints.
6. Assemble syringe expulsion system setup.
   1. Attach linear motion pillow blocks (mounting platforms + linear motion bearing) onto M8 chrome-plated stainless-steel rails (the parallel steel rails can be readily observed in **Figure 5**).
   2. Thread rails through linear shaft guide/support and lock rails. Use three guides per rail. Mount SE parts 1 and 2 onto pillow blocks using M4 machine screws.
   3. Loosely join SE parts 1 and 2 with M8 hex bolts. Configure the space between SE part 1 and 2 with helical compression springs covering each bolt that are secured between two inward facing nylon bushings (see **Figure 5F**). Mount these bushings on the exterior of the SE part 1 and SE part 2.

7. Wire circuit (see **Figure 6** for the core wiring diagram)
   1. Connect the motor controller to the I2C/SDA, 3.3 V, and GND pins on the single board computer.

Copyright © 2018 Journal of Visualized Experiments

2. Connect DC motor terminals to the M- and M+ blocks of the motor controller board. Connect the 24 V, 2.5 A power supply (**Figure 5B**) to the V+ and GND blocks of the motor controller (the controller is encased in a simple electronics box in the final design, see **Figure 5H**).
3. Connect the 3V3 and 5V pins of the motor control board to the respective pins on the single board computer. Connect SDA and SCL pins of the motor controller to pins 3 and 5 of the single board computer, respectively.
   Note: Commands are issued to the DC motor from the single board computer through a motor controller. Motor speed is controlled by regulating the voltage across the motor terminals via pulse width modulation. In this setup, the maximum current running through the 24 V DC motor (full-load amperage: 4.83 A) is limited to 2.5 A by the 24 V power supply. It is recommended that the motor circuit is wired through a normally-closed (NC) emergency stop (**Figure 5J**). Doing so provides a means to disrupt the motor circuit to enable a basic emergency shutdown operation.
4. Connect front and rear infrared proximity sensors (digital distance sensors, **Figure 5I**) to RPi GPIO pins 24 and 23, respectively.
   1. Route sensor wiring through conduits in the instrument base.
      Note: The IR sensors are non-contact break-beam motion sensors with a detection range of 2-10 cm.
   2. 4.7.4.2 Snap the wired IR sensors into 3D-printed infrared sensor braces (**Figure 5I**, black boxes) and mount onto the instrument base. When correctly set into the brace, the sensor face should protrude outwards from the 14 mm x 7 mm rectangular opening of the brace.
      Note: these sensor braces can be temporarily mounted using Velcro or an adhesive (temporary mounting is useful to appropriately adjust and optimize IR sensor placement). Alternatively, permanently mount by drilling small guide holes in the instrument base and securing the braces with M2 screws.

5. Connect a 7” touchscreen LCD display to the 5V, GND, and display serial interface (DSI) pins of the single board computer. The 7” RPi and LCD display assembly is shown in **Figure 5G**.

5. Fabricate Polymersomes via FNP Using the Custom-Made High-Speed Syringe Pump

1. (Option 1) Use auto run mode.
   1. Select **Auto Run** from the main menu. The system will prompt users to allow the motor to automatically position the syringe expulsion platform to the beginning of the precision slide. Ensure that the path in front of and behind the metal plate is clear prior to proceeding.
   2. Load 1 mL plastic syringes as described in section 2.5 and mount syringes onto the female Luer connectors of the CIJ mixer. Load CIJ mixer (with syringes attached) into the rectangular opening of the rear expulsion carriage (see **Figure 5E**).
   3. Set the desired motor speed (units: rpm) by using the slider in the GUI (see note below for important considerations). The optimal motor speed will depend on the specific pump and setup but must ensure a flow rate of at least 1 mL/s for the CIJ mixer channel dimensions provided here.
      Note: Consider the following while setting flow rate. In the vertical hand-operated FNP configuration, reactants are expelled from the syringes at a rate of ~1 mL/s, but can be highly variable when hand driven. This is simply the flow rate through the syringe barrel, which is controlled by the rate at which the user advances the syringe plunger. Note that the 1 mL/s rate is *not* referring to the exit flow rate from the smaller diameter nozzle. At the above specified channel dimensions, ~1 mL/s should be maintained to ensure an appropriate Reynold’s number for turbulent mixing[10]. Different flow rates can be used as long as the channel diameter is adjusted accordingly to maintain a Reynold’s number that supports turbulent conditions. The syringe plungers are advanced by a perpendicular metal plate, which moves along a high-precision aluminum slide coupled to the 24 V brushed DC motor. In this configuration, the maximum barrel flow rate is influenced by a number of factors, including (1) the maximum motor speed (4,252 rpm) and the screw lead of the precision slide (1.27 mm) that is coupled to the motor shaft (2) the torque of the motor (~0.2 N*m of full-load torque), which is needed to overcome resistance to flow (3) back pressure contributions from fluid entry into and exit from the CIJ mixer, and (4) the strength of the syringes used (users should be mindful of the forces acting on the syringes, and use syringes of appropriate strength). Regarding point (2), when increasing flow rate sufficient torque is required to avoid stalling the motor while maintaining steady expulsion under increasing back pressure. Barrel flow rates – to illustrate the barrel flow rate that the aforementioned system can achieve, consider the case where FNP is performed using reactants loaded into two one-milliliter syringes. To achieve a 1 mL/s flow rate through the barrel, the motor must advance the metal plate the distance defined by the plunger length (~68 mm for a typical one mL syringe) in one second. Provided the 1.27 mm screw lead of the precision slide, it follows that a DC motor operating at 4,252 rpm is capable of advancing the platform up to ~90 mm/s (71 rev/s*1.27 mm/rev). This corresponds to a barrel flow rate of ~1.3 mL/s, which exceeds the 1 mL/s target rate.
   4. Prior to running the instrument, check the system to ensure the that the path of the platform is clear of obstructions, and that the front and rear IR proximity detectors are clear of obstructions (the IR sensors are the small black boxes near the precision slide terminals; see **Figure 5I**). Also ensure that the capillary tubing outlet from the CIJ mixer is routed into an appropriate collection container (ex: glass beaker, *etc.*).
   5. To expel reactants from the syringes and into the CIJ mixer, press the **Run** button in the software interface.

2. (Option 2) Use manual run mode. Refer to the **Auto Run Mode** directions above and note the following change to step 5.1.5: press the forward button pressed continuously through the completion of the run (*i.e.,* the platform advances in response to an on-press event, and the motor will stop in response to an on-release event).
3. (Option 3) Use manual platform positioning mode; this mode allows users to position the platform by running the motor at low speed (20% power) in response to the forward and reverse buttons on the software interface.

Representative Results

Here, we have presented a simple protocol for the formulation of nanocarriers capable of loading hydrophilic and hydrophobic cargo that are safe for *in vivo* mouse and non-human primate administration[11,13]. We have also included a detailed protocol for the synthesis of the polymer used in our representative results, along with a description for the fabrication of a custom instrument for the mechanically-controlled impingement of solutions in the CIJ mixer. **Figure 1** provides an overview of the synthesis steps performed to produce PEG_{17}-*bl*-PPS_{35}-SH, the diblock copolymer used to self-assemble polymersome nanocarriers. An overview of the FNP protocol for assembling PEG-bl-PPS polymersomes loaded with therapeutics and/or imaging agents is diagramed in **Figure 2**. The polymer was impinged in a CIJ mixer (schematic shown in **Figure 3a**, originally described in [10]) to form monodisperse polymersomes as the aggregate morphology, which can be validated by dynamic light scattering (DLS) and cryogenic transmission electron microscopy (cryoTEM) (**Figure 3b-3c)**. Polymersomes formed by FNP become smaller (**Figure 3d**) and more monodisperse (**Figure 3e**) with subsequent impingements, and may be loaded with hydrophilic and hydrophobic cargo (*e.g.,* DiD lipophilic dye, small molecule therapeutics, protein *etc.*; **Figure 4a**). Nanocarriers formed under the sterile conditions described above are endotoxin free by both RAW Blue and LAL endotoxin assays and thus suitable for a wide range of *in vitro* and *in vivo* applications (**Figure 4b**, data not shown).

Lastly, we have designed and constructed an instrument to mechanically-control the flow rate and resulting impingement of solutions in the CIJ mixer (**Figure 5**). The creation of this instrument is essential, as commercially-available syringe pumps cannot achieve the flow rates needed for FNP. With the exception of custom modifications, commercially available syringe pumps have speed limitations imposed by their use of low-speed stepper motors, which are designed to reliably dispense fluid in a slow and steady fashion. In our instrument, reactant expulsion is controlled by a precision slide under the control of a 24 V brushed DC motor, which can achieve much greater speeds (4,252 rpm) than the slow stepper motors found in commercial syringe pumps. Custom software running on a single board computer is used to operate the instrument (**Figure 6**). 2D drawings have been provided in addition to 3D models of the parts. All drawings and models were created in FreeCAD (open-source parametric 3D CAD modeling software) to ensure that they are highly accessible to the research community. The software for operating the instrument was written in Python 2.7.12, allowing for the rapid development of custom FNP procedures to ensure the congruous production of nanocarriers (size, morphology, *etc.*). Software for operating the instrument will be made available upon request. Users should note that the software is not currently compatible with Python 3; however, this may change in future updates. By controlling reactant expulsion rate, this instrument eliminates the variable of human error from hand-operation.

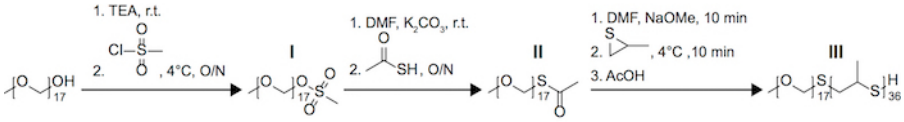

Figure 1. Synthesis schema for the synthesis of PEG_{17}-bl-PPS_{36}-SH. Please click here to view a larger version of this figure.

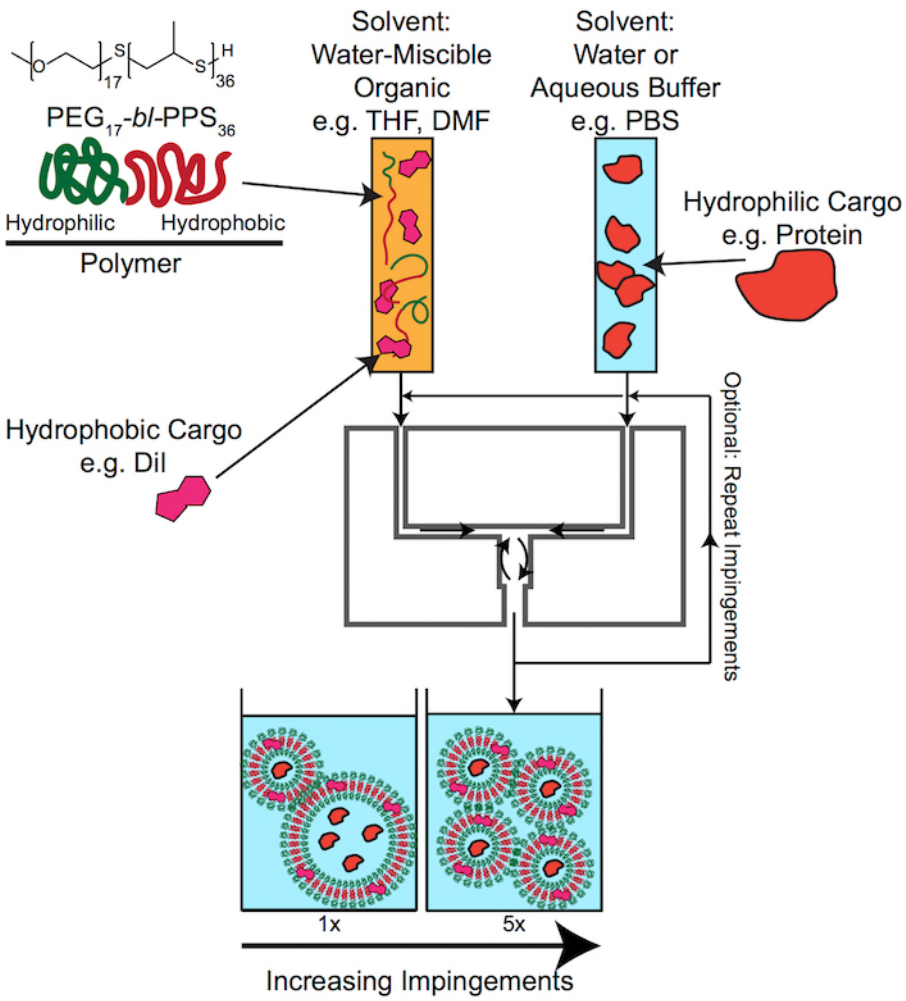

Figure 2. Production of polymersomes *via* FNP in a hand-driven CIJ mixer. Diagram of the formation of polymersomes using FNP. The PEG-bl-PPS polymer is dissolved in organic solvent along with hydrophobic cargo, and is impinged against aqueous solvent with dissolved hydrophilic cargo. Rapid mixing occurs within the CIJ mixer, and efflux can be repeatedly impinged or allowed to complete the formation process through dilution in a reservoir of aqueous solvent. Please click here to view a larger version of this figure.

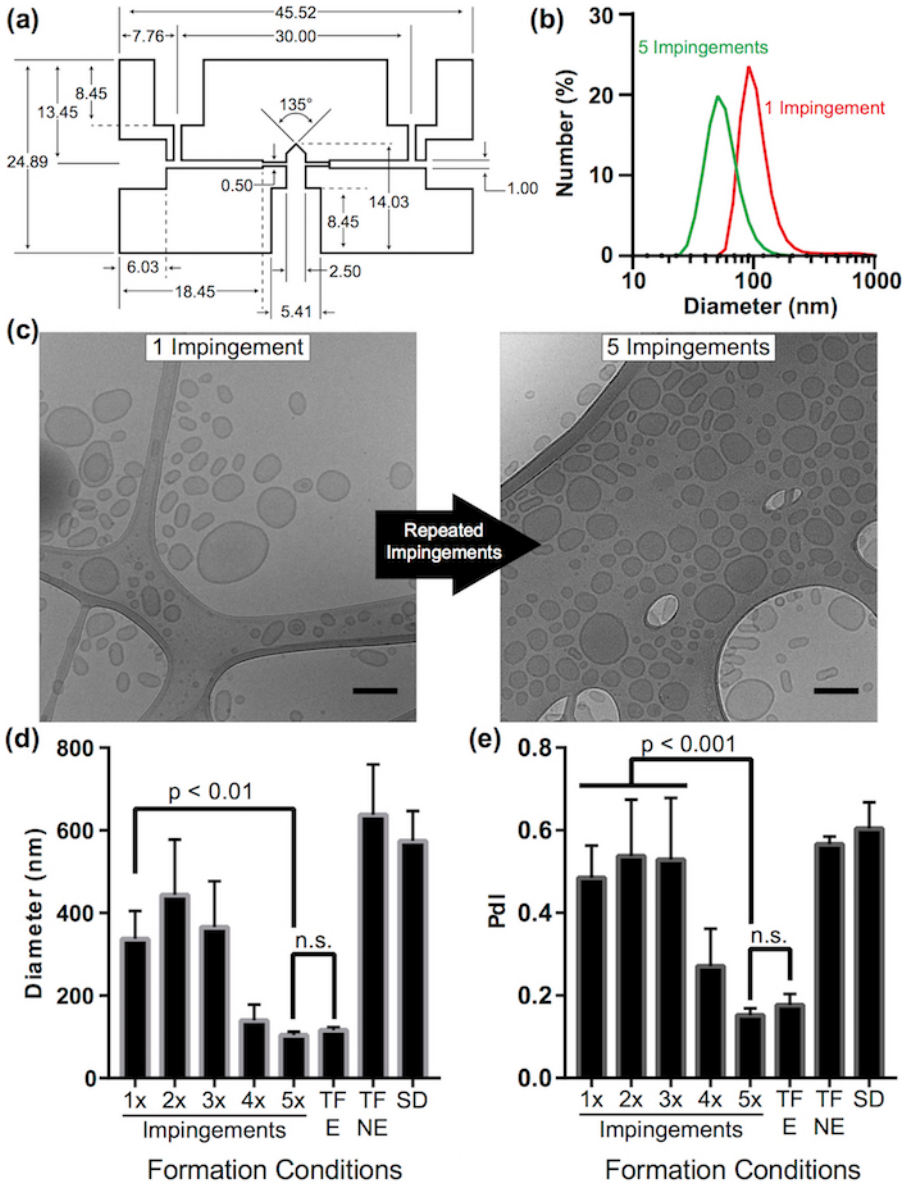

Figure 3. Characterization of polymersomes formed by FNP. (a) Design schematic of the CIJ mixer used in this study. All measurements are in millimeters. **(b)** Size distribution of polymersomes formed by FNP after 1 and 5 impingements, as measured by DLS. n = 6 formulations, mean of samples are graphed. **(c)** Example cryoTEM images of polymersomes formed after 1 and 5 impingements through the CIJ mixer, scale bar = 100 nm. Diameter **(d)** and polydispersity index **(e)** of polymersomes formed by FNP, measured by DLS. For comparison, polymersomes formed by thin film rehydration, with (TF-E) or without (TF-NE) subsequent extrusion, and formed by solvent dispersion (SD) were also measured, n=3, error bars represent standard deviation. Subfigures **(c)**-**(e)** taken with permission from Allen *et al.*[11]. Please click here to view a larger version of this figure.

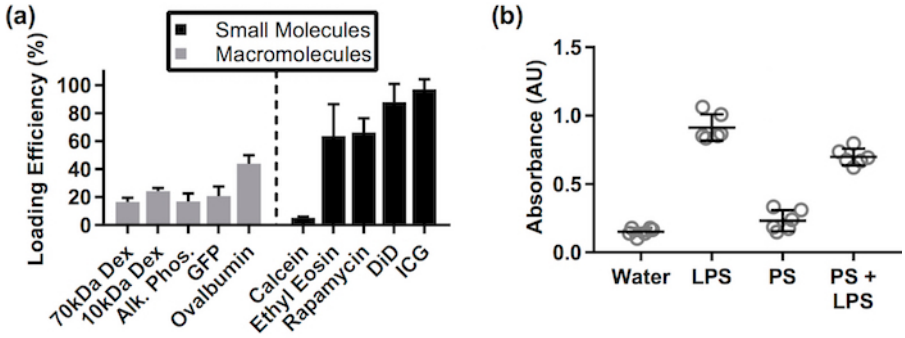

Figure 4. Loading efficiency and endotoxin characterization. (a) Loading efficiency of small and macromolecules within polymersomes, n=3, error bars represent standard deviation. **(b)** RAW Blue LPS assay of polymersomes formed by sterile FNP, n=6, error bars represent standard deviation. Please click here to view a larger version of this figure.

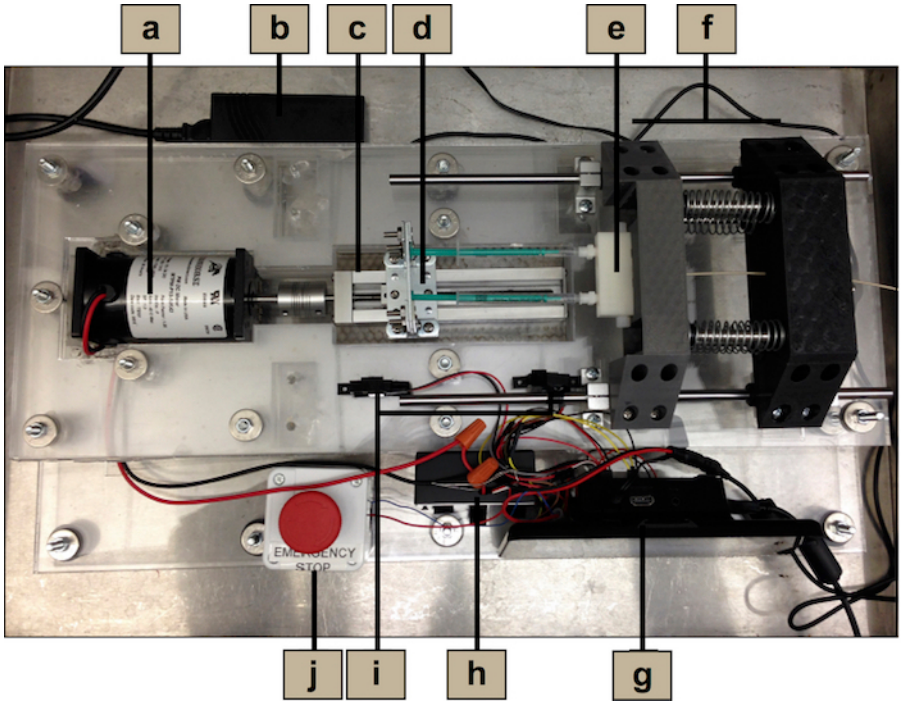

Figure 5. Instrument for the mechanical control of solution impingement in the CIJ mixer. (a) 24 V brushed DC Motor. **(b)** Power supply (24 V, 2.5 A). **(c)** 4.5" stroke precision slide with 1.27 mm screw lead (connected to motor shaft by a screw beam coupling). **(d)** Expulsion platform constructed from rectangular metal plates and L-shaped corner braces. **(e)** CIJ mixer. **(f)** Expulsion carriage. **(g)** single board computer and 7" touchscreen. **(h)** mMotor control board encased in plastic housing (83 mm x 53 mm x 35 mm). **(i)** IR sensors (non-contact break-beam motion sensors). **(j)** Emergency stop button (NC). Please click here to view a larger version of this figure.

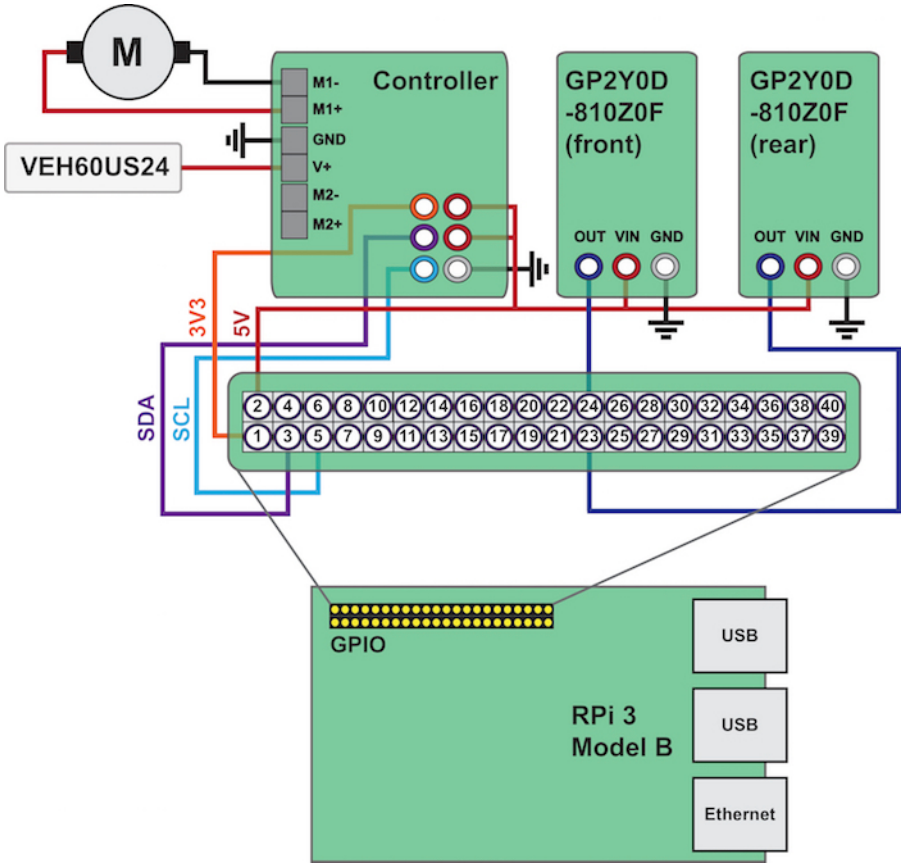

Figure 6. Core wiring diagram. The primary connections between the single board computer, motor controller, and IR sensors are displayed. The LCD touchscreen connections are not displayed here, as this component is non-essential (users may opt to use a standard computer monitor and mouse instead). Note that in the displayed configuration, the 24 V motor power supply and single board computer power supply are separate. Please click here to view a larger version of this figure.

Discussion

We have provided detailed instructions for the rapid fabrication of polymersomes using PEG_{17}-*bl*-PPS_{35}-SH as the diblock copolymer. Vesicular polymersomes are the primary aggregate morphology assembled at this ratio of hydrophilic PEG and hydrophobic PPS block molecular weight. When impinged multiple times, they have a diameter and polydispersity that matches polymersomes extruded through a 200 nm membrane after being formed *via* thin film hydration. This protocol thus eliminates the need for additional extrusion steps during the fabrication of monodisperse polymersome nanocarriers. Polymersomes formed *via* FNP load both hydrophilic and hydrophobic cargo, and maintain the bioactivity of those molecules through the formulation process[11]. Additional protocols are described to ensure sterility when necessary, allowing the formation of polymersome formulations that are endotoxin-free and therefore suitable for biochemical and immunological assays as well as safe for administration *in vivo*. The hand-operated CIJ mixer is simple to set up and provides ease-of-use to the user, but introduces potential quality control issues due to user variability. To maintain flow consistency, we sought to create an instrument capable of achieving and reproducibly maintaining a comparable flow rate. Importantly, at the above specified channel dimensions, commercial syringe pumps cannot achieve sufficiently high flow rates (~1 mL/s) due to being equipped with low speed stepper motors. To combat this issue, and to afford greater control over the flow rate, fabrication of a high-speed syringe pump for FNP was described. Care was taken to utilize open source and easily customizable software for the system OS and code.

Control over alternative flow rates offers the potential to fine-tune the nanocarrier formulation and provides opportunities to further explore the assembly of diverse nanocarrier morphologies. The Reynolds number and corresponding mixing time was previously shown to impact the size of solid-core nanocarriers formed via FNP[9], but it is not clear what impact it would have on the formation of polymersomes. This is a topic of current investigation, with the current recommended rate being 0.5 to 2 mL/s, with the representative results performed at approximately 1 mL/s. To increase control over flow rate even further, it may be necessary to replace the Linux-based OS with real-time control over the syringe pump motor.

Aside from adjusting the flow rate, there are a number of ways this FNP protocol can be modified to suite specific needs or applications. Smaller or larger amounts of polymer may be used. Concentrations as low as 1 mg/mL and as high as 100 mg/mL have been used to form stable nanocarriers. Larger volumes may be used for impingement, although consistent application of pressure during hand-driven FNP is more difficult at volumes greater than 1 mL per syringe. The volume of the reservoir may also be modified. Final organic:aqueous solvent ratios of greater than 1:3 may result in the incomplete formation of nanocarriers, and as such care should be taken to not decrease the volume of the reservoir without confirming the formation of nanocarriers. Aggregation may occur when attempting to load high concentrations of hydrophobic cargo, which can generally be alleviated by increasing the molar ratio of polymer:cargo.

Copyright © 2018 Journal of Visualized Experiments

An additional topic open for exploration is the further expansion of FNP polymersome formation to include other polymer systems beyond PEG-*bl*-PPS. Indeed, other systems have been used previously in the formation of micelles and solid-core drug nanocarriers[16,17]. However, it is not clear if there is a set of parameters that can lead to the formation of polymersomes *via* FNP using those other polymer systems. Given the number of potential variables to explore, it is entirely possible that other polymers can form polymersomes or other soft nanoarchitectures *via* FNP with adjusted experimental parameters, such as flow rate, temperature, solvent selection and polymer concentration.

As with all formulation techniques, there are limitations to FNP and restrictions that may make certain applications untenable. The rapid mixing process requires that the organic and aqueous solvents be miscible, which precludes the use of some common solvents used for the dissolution of many diblock copolymers, *e.g.,* dichloromethane and chloroform. Some polymers may therefore be rendered incompatible with FNP if they are not able to be dissolved in a water-miscible organic solvent. The FNP protocol described here utilizes a 1:1 ratio of organic to aqueous solvent, which may decrease the activity of payloads sensitive to high concentrations of organic solvent, such as some bioactive proteins. It should be noted that influences on bioactivity will depend on the protein, as we have previously found minimal effects on the enzymatic activity of alkaline phosphatase following loading within polymersomes by FNP[11]. Multi-inlet vortex mixers[18] are a more expensive but more customizable FNP platform that provides additional control over the ratio of organic to aqueous solvents, offering a versatile alternative to CIJ mixers for these contexts.

Disclosures

The authors declare that they have no competing financial interests.

Acknowledgements

We acknowledge staff and instrumentation support from the Structural Biology Facility at Northwestern University. The support from the R.H. Lurie Comprehensive Cancer Center of Northwestern University and the Northwestern University Structural Biology Facilities is acknowledged. The Gatan K2 direct electron detector was purchased with funds provided by the Chicago Biomedical Consortium with support from the Searle Funds at The Chicago Community Trust. We also thank the following facilities at Northwestern University: the Keck Interdisciplinary Surface Science Facility, the Structural Biology Facility, the Biological Imaging Facility, the Center for Advanced Molecular Imaging, and the Analytical Bionanotechnology Equipment Core. This research was supported by the National Science Foundation grant 1453576, the National Institutes of Health Director's New Innovator Award 1DP2HL132390-01, the Center for Regenerative Nanomedicine Catalyst Award and the 2014 McCormick Catalyst Award. SDA was supported in part by NIH predoctoral Biotechnology Training Grant T32GM008449.

References

1. Stano, A., Scott, E. A., Dane, K. Y., Swartz, M. A., & Hubbell, J. A. Tunable T cell immunity towards a protein antigen using polymersomes *vs.* solid-core nanoparticles. *Biomaterials.* **34** (17), 4339-4346 (2013).
2. Discher, B. M. *et al.* Polymersomes: tough vesicles made from diblock copolymers. *Science.* **284** (5417), 1143-1146 (1999).
3. Vasdekis, A. E., Scott, E. A., O'Neil, C. P., Psaltis, D., & Hubbell, J. A. Precision intracellular delivery based on optofluidic polymersome rupture. *ACS Nano.* **6** (9), 7850-7857 (2012).
4. Yi, S. *et al.* Tailoring Nanostructure Morphology for Enhanced Targeting of Dendritic Cells in Atherosclerosis. *ACS Nano.* **10** (12), 11290-11303 (2016).
5. Shum, H. C., Kim, J. W., & Weitz, D. A. Microfluidic fabrication of monodisperse biocompatible and biodegradable polymersomes with controlled permeability. *Journal of the American Chemical Society.* **130** (29), 9543-9549 (2008).
6. Pessi, J. *et al.* Microfluidics-assisted engineering of polymeric microcapsules with high encapsulation efficiency for protein drug delivery. *International Journal of Pharmaceutics.* **472** (1-2), 82-87 (2014).
7. O'Neil, C. P., Suzuki, T., Demurtas, D., Finka, A., & Hubbell, J. A. A novel method for the encapsulation of biomolecules into polymersomes via direct hydration. *Langmuir.* **25** (16), 9025-9029 (2009).
8. Saad, W. S., & Prud'homme, R. K. Principles of nanoparticle formation by flash nanoprecipitation. *Nano Today.* **11** (2), 212-227 (2016).
9. Johnson, B. K., & Prud'homme, R. K. Mechanism for rapid self-assembly of block copolymer nanoparticles. *Physical Review Letters.* **91** (11), 118302 (2003).
10. Han, J. *et al.* A simple confined impingement jets mixer for flash nanoprecipitation. *Journal of Pharmaceutical Sciences.* **101** (10), 4018-4023 (2012).
11. Allen, S., Osorio, O., Liu, Y. G., & Scott, E. Facile assembly and loading of theranostic polymersomes via multi-impingement flash nanoprecipitation. *Journal of Controlled Release.* **262** 91-103 (2017).
12. Bobbala, S., Allen, S. D., & Scott, E. A. Flash nanoprecipitation permits versatile assembly and loading of polymeric bicontinuous cubic nanospheres. *Nanoscale.* **10** (11), 5078-5088 (2018).
13. Allen, S. D. *et al.* Polymersomes scalably fabricated via flash nanoprecipitation are non-toxic in non-human primates and associate with leukocytes in the spleen and kidney following intravenous administration. *Nano Research.* (2018).
14. Karabin, N. B. *et al.* Sustained micellar delivery via inducible transitions in nanostructure morphology. *Nature Communications.* **9** (1), 624 (2018).
15. Mascoli, C. C., & Weary, M. E. Limulus amebocyte lysate (LAL) test for detecting pyrogens in parenteral injectable products and medical devices: advantages to manufacturers and regulatory officials. *Journal of the Parenteral Drug Association.* **33** (2), 81-95 (1979).
16. Pustulka, K. M. *et al.* Flash nanoprecipitation: particle structure and stability. *Molecular Pharmaceutics.* **10** (11), 4367-4377 (2013).
17. Tang, C., Amin, D., Messersmith, P. B., Anthony, J. E., & Prud'homme, R. K. Polymer directed self-assembly of pH-responsive antioxidant nanoparticles. *Langmuir.* **31** (12), 3612-3620 (2015).
18. Gindy, M. E., Panagiotopoulos, A. Z., & Prud'homme, R. K. Composite block copolymer stabilized nanoparticles: simultaneous encapsulation of organic actives and inorganic nanostructures. *Langmuir.* **24** (1), 83-90 (2008).

Copyright © 2018 Journal of Visualized Experiments